

derivatives.⁶ This strongly suggests that stabilization of the αN_1 tautomer in His^- does not result from hydrogen bonding between the primary amine protons and βN_3 of the imidazole ring but rather may be largely attributable to electronic or steric consequences of substitution at C_4 . In His^\pm , on the other hand, the decreased stabilization of the βN_1 tautomer may be indicative of significant hydrogen bonding between the primary aminium protons and βN_3 of the imidazole ring. In view of the greater overall consistency of all the results, it seems to us that $J_{\text{C}_5\text{N}_1}$ may be the parameter best suited for estimation of tautomeric abundances in these systems.

Conclusions

It is perhaps surprising that ring coupling constants in the imidazole derivatives are so closely similar to those in imidazole itself. However, as the calculated values reflect similar behavior, and correspondence with observed coupling constants for equivalent bonds in such divergent structures as pyrrole and pyridine is quite good (Table IV), it must be concluded that they are not really sensitive indicators of structural features other than protonation or deprotonation of the pyridine-like nitrogen (N_3). While it is tempting to rely more heavily on ^{15}N chemical shifts or NH couplings as indicators for such protonation or deprotonation, it should be noted that for NH couplings the range of values between protonation extremes is relatively small and for ^{15}N shifts effects of the extramolecular environment can be large.^{10,11} It therefore seems that $^1J_{\text{CN}}$ may be the NMR parameter best suited for estimating the degree of protonation of imidazole-ring N_3 under the most general conditions.

The largest discrepancies noted in this work are between the

observed and calculated values for $J_{\text{C}_4\text{N}_1}$ and $J_{\text{C}_2\text{N}_3}$ in 1-methylimidazole. As the observed values do not appear to be solvent dependent to any appreciable extent and the calculated values do not change significantly upon incorporation of hydrogen-bonded structures, we are unable to suggest a resolution for the discrepancies.

Acknowledgment. This work was performed under the auspices of the U.S. Department of Energy.

References and Notes

- (1) (a) The Los Alamos Scientific Laboratory. (b) The University of Texas.
- (2) (a) Sundberg, R. J.; Martin, R. B. *Chem. Rev.* **1974**, *74*, 471 (cf. p 495). (b) Bachovchin, W. W.; Roberts, J. D. *J. Am. Chem. Soc.* **1978**, *100*, 8041.
- (3) Alei, M., Jr.; Morgan, L. O.; Wageman, W. E. *Inorg. Chem.* **1978**, *17*, 2288, 3314.
- (4) Wasylishen, R. E.; Tomlinson, G. *Biochem. J.* **1975**, *147*, 605.
- (5) Wasylishen, R. E.; Tomlinson, G. *Can. J. Biochem.* **1977**, *55*, 579.
- (6) Reynolds, W. F.; Peat, I. R.; Freedman, M. H.; Lyerla, J. R., Jr. *J. Am. Chem. Soc.* **1973**, *95*, 328.
- (7) Reynolds, W. F.; Freedman, M. H. *J. Am. Chem. Soc.* **1974**, *96*, 570.
- (8) Kawano, K.; Kyogoku, Y. *Chem. Lett.* **1975**, 1305.
- (9) Blomberg, F.; Maurer, W.; Rüterjans, H. *J. Am. Chem. Soc.* **1977**, *99*, 8149.
- (10) Alei, M. Jr.; Wageman, W. E. *Tetrahedron Lett.* **1979**, 667-670.
- (11) Schuster, I. I.; Roberts, J. D. *J. Org. Chem.* **1979**, *44*, 3864.
- (12) Nicolet Instrument Corp., NIC-05-40417, revised Sept 1972.
- (13) Pople, J. A.; Schneider, W. G.; Bernstein, H. J. "High Resolution Nuclear Magnetic Resonance", McGraw-Hill, New York, 1959.
- (14) Becker, E. D. "High Resolution NMR", Academic Press, New York, 1969.
- (15) Alei, M. Jr.; Florin, A. E. *J. Phys. Chem.* **1968**, *72*, 550.
- (16) Schulman, J. M.; Venanzi, T. *J. Am. Chem. Soc.* **1976**, *98*, 4701, 6739.
- (17) Blizzard, A. C.; Santry, D. P. *J. Chem. Phys.* **1971**, *55*, 950.
- (18) Wang, S. M.; Li, N. C. *J. Am. Chem. Soc.* **1966**, *88*, 4592.
- (19) Lichter, R. L.; Roberts, J. D. *J. Am. Chem. Soc.* **1971**, *93*, 5218.
- (20) Kintzinger, J. P.; Lehn, J. M. *Chem. Commun.* **1967**, 660. *Mol. Phys.* **1968**, *14*, 133.
- (21) London, R. E. *J. Chem. Soc., Chem. Commun.* **1978**, 1070.

Electronic Spectra and Structure of a Weak π Complex. Vibronic Structure in the Charge-Transfer Transition of Anthracene-*s*-Trinitrobenzene

C. J. Eckhardt^{†*} and H. Eckhardt

Contribution from the Department of Chemistry, University of Nebraska, Lincoln, Nebraska 68588. Received August 20, 1979

Abstract: Polarized specular reflection and absorption spectra for the crystalline anthracene-*s*-trinitrobenzene complex are reported at 20 and 5 K. The quantitative assignment of the polarization of the CT transition of the asymmetric complex places the moment near the line-of-centers. An irregular vibrational progression of $\sim 1400\text{ cm}^{-1}$ is observed for the CT transition. A second CT band is observed at $31\,000\text{ cm}^{-1}$. The first and second singlet transitions of anthracene are observed and are found to have free molecule frequencies, intensities, and polarizations. A band seen at $44\,000\text{ cm}^{-1}$ is interpreted as a trinitrobenzene molecular transition. The use of crystals of complexes for study of molecular spectra is suggested.

I. Introduction

Recent work in our laboratory has been concerned with the electronic spectra and structure of electron donor-acceptor (EDA) complexes in crystals.¹⁻³ In an effort to further understand the nature of this interaction, we have been particularly concerned with the effects of varied acceptors with a specific donor molecule, namely, anthracene. Previous studies of anthracene crystalline complexes with TCNQ⁰¹ and pyromellitic dianhydride^{2,4} have been made with detailed examination of the excitonic interactions of the latter reported

by other workers.^{5,6} The concern in our investigations has been centered, insofar as possible, upon the molecular manifestation of the EDA interaction.

The complex of 1,3,5-trinitrobenzene (TNB) with anthracene (A) is one which has been extensively studied. Early work on the complex was done in solution and in organic glasses.⁷⁻⁹ Later work on crystalline films of TNB-A^{10,11} was reported but, since such a study for a single crystal orientation cannot absolutely assign the charge-transfer (CT) transition moment in this asymmetric complex, further study is necessary to obtain the assignment. Below is shown the projection of TNB onto the plane of A.

[†] John Simon Guggenheim Fellow, 1979-1980.

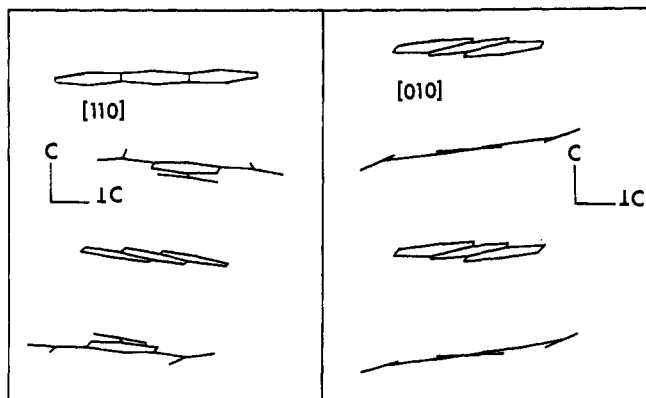
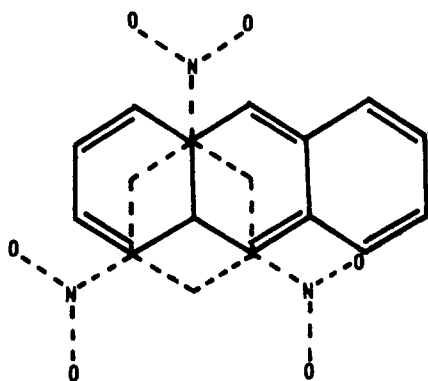


Figure 1. Projections of A-TNB onto (110) and (010).



First-order theory for a 1:1 EDA complex¹² predicts the polarization of the CT transition to be along the line of centers of the donor and acceptor molecules. For $n:n$ EDA complexes such as those found in crystals, this has also been found,^{1-4,13} but in these, as well as other cases, the crystal packing has always been such that the optimum geometry, the typical herringbone stack, has had a crystal axis along its line-of-centers, thus assuring the expected CT polarization. The TNB-A complex, however, differs in that the TNB molecules above and below a given A are at opposite ends of the A and each A is rotated 120° to its neighboring A molecule in the stack. The lines-of-centers do not then coincide with any symmetry operation of either the crystal or complex. Thus, the possibility exists that the CT moment may deviate from the expected polarization.

Another purpose of the investigation is the examination of the effect of complexation upon the transitions of the donor. Further interest centers upon the vibrational structure in the CT band. Such structure in CT bands in solution is infrequent¹⁴ but is more commonly seen in EDA complex crystals.

This paper reports the electronic spectra of the TNB-A complex at 300, 20, and 5 K from 10 000 to 46 000 cm^{-1} . Assignments of CT transition moments as well as intramolecular anthracene transition moments are made. The origins of the transitions are discussed and compared with other anthracene EDA complexes. The influence of the crystalline environment is also considered.

II. Experimental Section

A. Sample Preparation. TNB obtained from Eastman Organics was recrystallized from chloroform. Blue-violet fluorescence anthracene obtained from the same supplier was used without further purification. The EDA crystals were prepared by combining separate solutions (ethanol or diethyl ether) of the donor and acceptor and obtaining crystals of the complex by evaporation. Those crystals obtained from the ether were larger and possessed better morphology than those grown from ethanol but they were otherwise of identical structure.

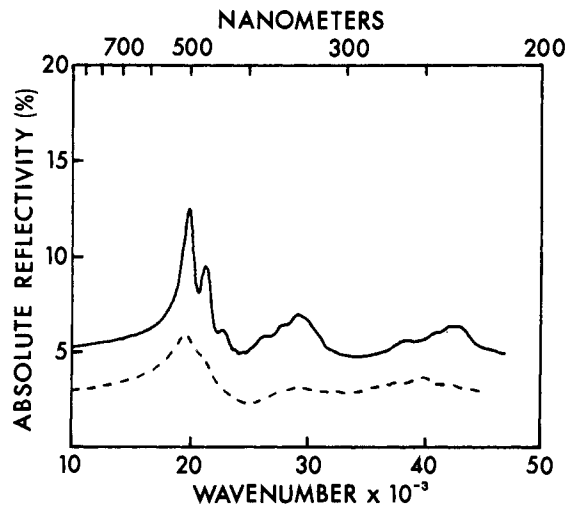


Figure 2. c axis polarized reflection spectra at 300 (---) and 5 K (—).

Table I. Frequencies of Prominent Structure in the Polarized Spectra of A-TNB

$C_{\perp}(010)$	$C_{\perp}(110)$	C_{\parallel}
20 470	20 270	20 320
		21 750
21 650	21 710	
	23 080	23 030
		24 550
26 670	26 670	
28 010	28 020	
29 370	29 370	
30 930	30 670 (sh)	
		31 450
38 910	38 350	
39 670 (sh)	38 840 (sh)	
39 870 (sh)	39 730 (sh)	
44 000		

B. Spectroscopic Measurements. Reflection spectra were obtained at both 300 and 2 K with apparatus used in previously reported work.^{1,15}

Absorption spectra were obtained by a microspectrophotometer similar to that described by Fratini and Anex.¹⁵ The films were prepared by melting crystals of the complex between two fused silica cover slips which were pressed together. The resulting film was polycrystalline wherein the areas displayed distinct dichroism with orthogonal principal directions. The film thicknesses were measured to ± 100 Å by interferometric measurement. No significant dispersion of the principal directions was observed for the faces studied.

C. Crystal Morphology and Projections. The monoclinic acicular crystals are zonal to the c axis.¹⁶ Faces determined by optical goniometry were {010}, {110}, and $\{\bar{1}10\}$. Projections of the molecules onto two faces are shown in Figure 1. Because two of the complex molecules in one column of the TNB-A unit cell are related to two molecules in the other column by c -face centering, it is only necessary to consider the projections of the molecule in one column. It is clear that the individual 1:1 complex possesses no symmetry.

III. Results

A. Spectra. The reflection spectra taken with light polarized along the c axis at both 300 and 5 K are shown in Figure 2. Significant sharpening of the structure in the low-energy c -axis system is observed at low temperature. Frequencies of prominent structure are listed in Table I. At 300 K only shoulders are observed.

The Kramers-Kronig transforms of the low-energy c -axis system are shown on the left side of Figure 3 at 300 and 6 K. The $\sim 1400\text{-cm}^{-1}$ progression observed in the reflection spectrum is preserved. However, not enough resolution of

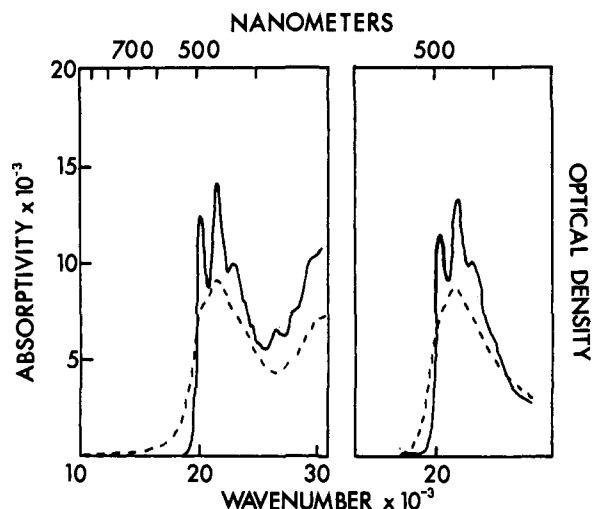


Figure 3. *c* axis polarized spectra at high (---) and low (—) temperature. Left side shows the Kramers-Kronig transform of the visible region. The right side displays the thin film absorption spectra over the visible region.

Table II. Vectors for CT Moment from Experimental Data for Anthracene-TNB

method	vector	angle to <i>c</i> axis, deg
average	(-0.6714, 0.4173, 0.6408)	22.1
weighted average	(-0.6327, 0.4175, 0.6621)	23.7
line of center	(-0.6325, 0.3651, 0.6831)	21.4

structure is obtained to allow meaningful definition of any other vibrational series. On the right side of Figure 3 are displayed the direct film absorption spectra for the *c*-axis polarization at 300 and 20 K. The agreement with the transformed spectra is excellent.

Another system is observed at 29 000 cm^{-1} but it is rather broad and diffuse. A weak and broad system is also observed at 44 000 cm^{-1} but, because its reflectivity has varied significantly between measurements, it has not been considered further.

The crystal directional intensity, q_{xl}^2 , which is taken to be the spherical average of the crystal integrated intensity observed along a given principal direction, is 0.19 \AA^2 for the *c*-axis polarized band in the visible at 6 K; at 300 K the value is 0.17 \AA^2 .

The reflection spectra obtained at 6 K with light polarized perpendicular to the *c* axis (C_{\perp}) in the (010) and (110) faces are shown in Figures 4 and 5. Their respective Kramers-Kronig transforms are shown in the same figures. From these spectra it is clear that a dichroism exists in the visible region and that the structure in this region corresponds to the region of the *c*-axis absorption. Further, the structure which appears from 20 000 to 23 000 cm^{-1} shows a $\sim 1400\text{-cm}^{-1}$ progression. Table I lists the frequencies of prominent structure.

B. Assignment of Transitions. Since there are four complexes in the $C2/c$ unit cell,¹⁶ it is emphasized that the individual complexes have no symmetry. There are, therefore, no symmetry constraints on the CT transition and its assignment must be made from at least two sets of spectra taken from geometrically inequivalent but possibly spectroscopically equivalent faces.

The dichroic ratios measured for a given face determine two possible projectors of a transition moment in the unit cell upon that face. One of these projectors¹⁷ must lie in a plane which contains the transition moment but which is perpendicular to the face containing the projectors. The intersection of the planes actually containing the transition moment and the

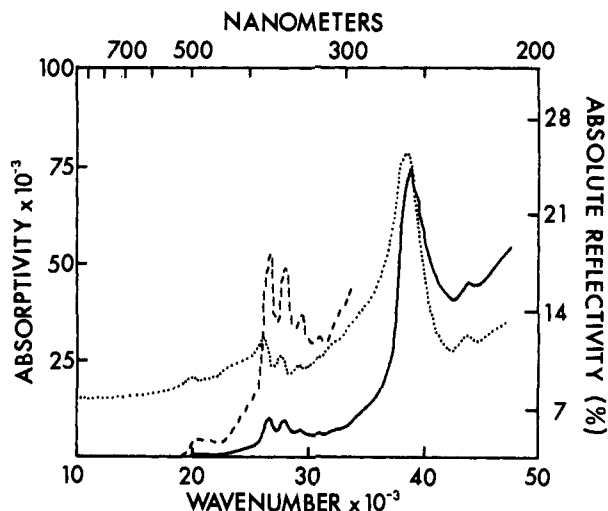


Figure 4. C_{\perp} axis polarized reflection spectra (....) and their Kramers-Kronig transforms (—) for {010}. The dashed lines represent blow-ups of structure by a factor of 5.

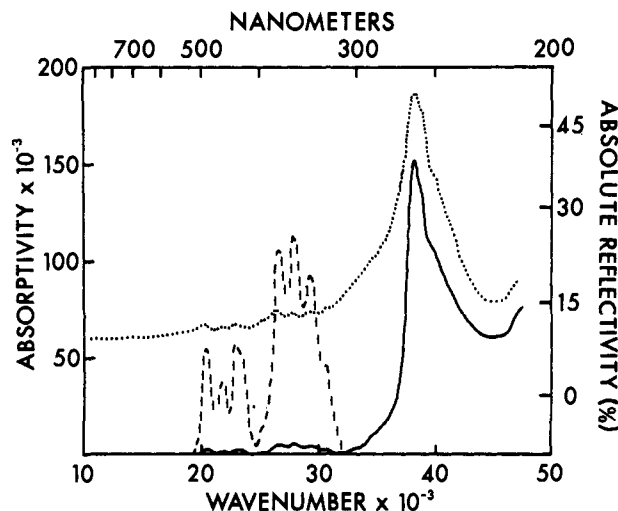


Figure 5. C_{\perp} axis polarized reflection spectra (....) and their Kramers-Kronig transforms (—) for {110}. The dashed lines represent blow-ups of structure by a factor of 20.

various projectors will define a vector parallel to that moment. Thus spectra must be obtained from a minimum of two geometrically inequivalent faces. Because some of the possible projectors arise because of sign ambiguity, intersections will be obtained which will be devoid of physical significance.

The observed dichroic ratio for the low-energy system, which has been previously assigned qualitatively as a CT transition,^{10,11} is for (110) $C/C_{\perp}^{110} = 7.4$. This is also the ratio for the spectroscopically equivalent but geometrically inequivalent (110) face. For (010) the dichroic ratio is $C/C_{\perp}^{010} = 32$, which for practical purposes may be taken to be infinite.

Using these data according to the previously described analysis yields a set of five vectors which are physically reasonable for a CT transition in an $a\pi-b\pi$ type complex. Slightly different intersections and thus possible moments are obtained because of experimental error. The "average" CT transition moment vector was obtained in two ways: (1) the average of the vector components was obtained and (2) a weighted average was taken with each component weighted inversely to the square of its deviation from the average component. The resultant values are shown in Table II. Because of the *c*-face centering and the location of the component molecules at special positions, the stacks of complexes are identical. This,

coupled with the symmetric arrangement of the line-of-centers to the c axis, facilitates the calculation and assignment of the CT transition moment.

Using the above experiments' polarization assignment, the absolute intensity of the CT transition in the crystal may be obtained. At low temperature the integrated intensity is 0.212 \AA^2 and at ambient it is 0.192 \AA^2 as determined from the Kramers-Kronig transforms. The integrated intensity obtained from the film spectra which are of (110) orientation¹¹ is 0.182 \AA^2 at low temperature. Film thickness was determined interferometrically. The above values take into account the doubled cross section of the CT transition for a given donor in a stack.¹¹ The peak absorptivity at 300 K is $1570 \text{ L/mol}\cdot\text{cm}$, which is in reasonable agreement with earlier measurement of $1980 \text{ L/mol}\cdot\text{cm}$.

The intensity of this CT transition in chloroform was determined, without modifying assumptions,¹⁹ to have a peak absorptivity of $2000 \text{ L/mol}\cdot\text{cm}$. Peak extinction was reported to be $1333 \text{ L/mol}\cdot\text{cm}$ in a Benesi-Hildebrand determination.²⁰ A value of $1600 \text{ L/mol}\cdot\text{cm}$ is reported for ethyl ether-pentane-alcohol mixed solvent.⁸ Thus, there is an apparent solvent dependence on the CT intensity. Because of this, the intermediate value of $1600 \text{ L/mol}\cdot\text{cm}$ is selected. Using this, the integrated intensity using a Gaussian approximation for the solution spectrum band shape is 0.163 \AA^2 , which is in good agreement with the intensity found in the crystal considering the approximation involved. A similar approximate determination¹⁰ reports a cross section of 0.130 \AA^2 and use of the Gaussian band shape approximation for these data gives a dipole strength of 0.182 \AA^2 . Considering the errors inherent in the Benesi-Hildebrand procedures,²¹ the agreement is quite satisfactory.

The low-temperature crystal CT transition intensity is 28% greater than that at ambient temperature. This hyperchromism is attributed to contraction of the crystal and resulting increase of chromophore concentration. Because this will also result in an increase of overlap between the donor and acceptor molecules, the CT intensity can also be expected to increase. Both bathochromic and hyperchromic changes in the A-TNB complex at 16 kbar and 300 K have been observed.²²

The nature of the weaker reflection in the c -axis spectrum which is observed at about $31\,000 \text{ cm}^{-1}$ has been previously assigned¹¹ as a second CT transition. Because of overlap with known anthracene transitions in this energy region in the C_{\perp} spectra further analysis using dichroism is thwarted. The integrated crystal directional intensity is 0.12 \AA^2 .

For the C_{\perp} spectra in the $19\,700\text{-cm}^{-1}$ CT region, vibrational structure is observed clearly only for $\{110\}$ and $\{\bar{1}10\}$. The $\{010\}$ spectra for this direction are too diffuse. In Table I are listed the frequencies of prominent structure in this region. These data support previous arguments for excitonic interaction¹¹ but the magnitude of the factor group splitting here is certain to only $\pm 80 \text{ cm}^{-1}$ since the estimated error in the assigned frequencies for peaks is $\pm 40 \text{ cm}^{-1}$.

The C_{\perp} spectra at low temperature (Figure 4) are dominated by the first and second singlet transitions of anthracene. These are known to be polarized along the short and long axes in the free molecule, respectively,²³ and this is expected in the A-TNB complex. Because the c axis is nearly perpendicular to the anthracene plane, the dichroic ratios C/C_{\perp} for the faces are of little use. However, the intensity ratios between any two principal directions may be used for making an assignment. In A-TNB the intensity ratios between the C_{\perp} polarizations should vary with the face and the polarization of the transition moment. Because of the symmetry requirements on the anthracene transitions and their known polarizations, only the ratios for the long and short axes need be known. For the short axis $C_{\perp}^{010}/C_{\perp}^{110} = 2.4$ and for the long axis the ratio is 0.32. Because the anthracene singlet transitions must be confined

to the molecular plane, the detailed analysis used for the CT transition is unnecessary.

For S_1 in anthracene in the region from $25\,000$ to $31\,000 \text{ cm}^{-1}$, $C_{\perp}^{010}/C_{\perp}^{110} = 2.2$, which is in excellent agreement with theory. The integrated intensity obtained from Kramers-Kronig transform (Figure 4) for S_1 on (010) is 0.28 \AA^2 and (110) is 0.32 \AA^2 . The solution intensity in hexane for anthracene's S_1 was found to be 0.31 \AA^2 . This agreement between solution and crystal values is well within the estimated error of 5%.

For the S_2 intensity measured between $31\,000$ and $42\,000 \text{ cm}^{-1}$, $C_{\perp}^{010}/C_{\perp}^{110} = 0.32$, which is also the theoretical value for a long axis polarized transition. The integrated intensity for S_2 as determined from (010) is 3.95 \AA^2 and from (110) is 4.00 \AA^2 . The solution value is 3.72 \AA^2 . A weak and diffuse absorption ($\epsilon \sim 10^3$) at $35\,700 \text{ cm}^{-1}$ for TNB in n -heptane is observed and the discrepancy in crystal and solution intensities for S_2 may be ascribed to this. The observed frequency difference between the S_2 peaks for (101) and (110) may be attributed to this absorption as well as the more intense ($\epsilon \sim 10^4$) $\pi^* \leftarrow \pi$ TNB transition at $45\,000 \text{ cm}^{-1}$.

The peak observed at $44\,000 \text{ cm}^{-1}$ in the C_{\perp}^{010} spectrum cannot be assigned because of the lack of any reasonable way to obtain an intensity ratio for the band. It is taken to be electronic in origin since it is more than 4000 cm^{-1} to the blue of S_2 and is not seen in C_{\perp}^{110} . The high intensity of S_2 on (110) may be expected to obscure any weaker structure nearby. The band in question is of such significant intensity that, were it long axis polarized, it would appear as a peak or shoulder at $44\,000 \text{ cm}^{-1}$ on S_2 in (110). Since this is not observed, a reasonable inference would be that the transition has a short axis polarization. This is further supported by the observation that short axis transitions project strongly onto (010) and weakly onto (110).

There is no strong evidence for factor group splitting in the anthracene bands. This, coupled with the excellent agreement of crystal and solution intensities and frequencies, supports the oriented gas model for the crystal for description of the anthracene transitions.

IV. Discussion

The agreement of the experimental CT transition polarization with the prediction of Mulliken's theory for polarization along the line-of-centers for 1:1 complexes is excellent. The situation differs from other studies on crystalline CT complexes where the line-of-centers and the stacking axis are coincident. It is in these systems where significant shifts of the CT frequency and intensity from that observed in solution are often observed.^{1,3,4} A-TNB, however, appears to behave as a 1:1 complex and it is intriguing to consider, given the exact agreement of the maximum frequency of absorption between crystal and solution as well as their agreement in integrated intensities, that the geometries of the complex in the two phases might be the same.

These measurements quantitatively establish the qualitative assignment of the polarization of the first CT transition made earlier.^{10,11} Further, they establish the usefulness of intensity ratios between principal directions in different faces for the oriented gas model of a crystal.

Of most interest in the CT system is the clear definition of the vibrational progression in the CT band. Unfortunately, even with spectra which are apparently better resolved than those reported earlier,^{10,11} it has not been possible to identify (Table I) more than a $\sim 1400\text{-cm}^{-1}$ progression. However, this is of higher frequency than the progression reported in the crystal fluorescence^{10,11} by approximately 100 cm^{-1} . Of course, neither of these is a pure vibrational frequency. This supports the conclusion that the nature of the fluorescing complex is altered from that undergoing absorption.¹¹ The

study of the polarized fluorescence from different faces and subsequent assignment of the CT emission's polarization can be expected to elucidate the nature of the geometry change the highly polar excited state suffers in the lattice.

The 31 000-cm⁻¹ band has been argued¹¹ to be a CT transition from the penultimately filled orbital (PFO) of anthracene to the LUMO of TNB. The energy difference in the centers of gravity of the low-energy CT band and that in question is 9200 cm⁻¹. It was pointed out¹¹ that the calculated²⁵ difference between the LUMO and PFO is 8200 cm⁻¹ and should thus be close to the difference of energies between the two CT transitions. The 12 000-cm⁻¹ transition of the anthracene mononegative ion²⁶ is also used to support the assignment. Photoelectron spectroscopy shows the vertical ionization energies for the anthracene HOMO and PFO to differ by 9000 cm⁻¹.²⁶ Of course, correlation will slightly affect these energies since the distribution of electrons in the complex will be different than in the anthracene.

Multiple CT bands have been observed in other $a\pi$ - $b\pi$ complexes of anthracene. In the A-TCNQ complex, the lowest energy CT transition is from the PFO of A to the LUMO of TCNQ,¹ thereby preventing determination of the energy difference relevant to this assignment. In the crystalline complex of A with pyromellitic dianhydride (PMDA)^{2,4} a second transition is observed at 30 000 cm⁻¹ which is largely polarized out of the plane of the anthracene. In contrast to the previous two anthracene complexes, the first CT transition in A-PMDA crystal at 18 700 cm⁻¹ is red shifted from the solution value by 1600 cm⁻¹. However, the 30 000-cm⁻¹ band is in the same energy region as that observed in A-TNB and likely has the same origin.

In all of these complexes, the role of vibrational structure in the CT bands is of particular interest. In both A-TNB and A-PMDA it is quite prominent for the first CT band but in both complexes the second CT band remains diffuse. In A-TCNQ, there is no indication of such structure in the room temperature spectra.

The very strong 1400-cm⁻¹ progression observed in S₁ of anthracene has been attributed to a C-C stretch of either a_g or b_{3g} symmetry.²⁷ In A-TNB, the low-energy CT band remarkably resembles S₁ of anthracene both in shape and frequency interval. This is suggestive that the same vibration is active in the CT transition as in the anthracene S₁. The vibration should be affected by the CT interaction since partial or total removal of an electron from the HOMO of anthracene, a sacrificial donor, will cause a weakening of the C-C bonds and decreasing vibrational frequency. Thus, a similar decrease is expected in the anthracene S₁ in the complex and, as shown in Table I, is observed to be of essentially the same value as that observed for the CT band. However, the reflection spectrum of TNB crystals at 25 K shows a weakly defined progression of ~1400 cm⁻¹ in a system at 37 000 cm⁻¹ which, from its intensity, may be assigned as a $\pi^* \leftarrow \pi$ transition. This C-C stretch is presumably that which is active in $\pi^* \leftarrow \pi$ transitions in benzenoid systems and varies only slightly between molecules. Unfortunately, the lack of definition of the TNB progression prevents further analysis.

Since a ~1400-cm⁻¹ progression is observed in the lowest A-PMDA CT band, it is likely that the same C-C stretch is active in the lowest singlet of the acenes as is active in CT transitions of those EDA complexes which are comprised of benzenoid donors and acceptors. That this is possibly not a pure vibrational progression must be emphasized. The strength of the progression in the CT bands and its dominance in the acenes²⁸ and anthracene²⁹ in particular strongly support the C-C stretch as the active mode.

The intramolecular S₁ and S₂ transitions of anthracene are essentially unaffected by the EDA interaction. No excitonic effects are observed and the band shapes, intensities, and

frequencies are those of the free molecule in solution.

The origin of the 44 000-cm⁻¹ peak cannot be assigned. LCAO-MO-SCF-CI calculations²³ would indicate that from its energy the band could be a long axis polarized transition to a B_{1g} state of anthracene. The apparent experimental polarization, although uncertain, does not support such assignment. The $\pi^* \leftarrow \pi$ in TNB is of the correct frequency also. The TNB molecules are at sites of C₂ symmetry with the rotation axis parallel to the crystal *b* axis. Thus the molecular point group symmetry is lowered from D_{3h} to C₂. In fact, the nitro group which lies on the twofold axis²⁴ is twisted out of the plane of the molecule. The EDA interaction may be viewed as partial donation of an electron into the acceptor LUMO, and, since this orbital is degenerate in TNB,³⁰ a Jahn-Teller type distortion may be expected. The effect is further complicated by the fact that removal of an electron from the triply degenerate (E", A₁"') set of HOMOs will also cause Jahn-Teller distortion. ESR spectra indicate the presence of such distortion for the radical anion of TNB.³¹ It is not possible to predict the polarization of the $\pi^* \leftarrow \pi$ on TNB by symmetry correlation arguments alone and calculation of the C₂ symmetry TNB molecule is required. However, the transition in question must either lie along the *b* axis or perpendicular thereto and consideration of the orbitals involved indicates that the transition could easily be "short axis" polarized. Since the crystal data and available information are not in conflict, the suggested assignment for the 44 000-cm⁻¹ band is the $\pi^* \leftarrow \pi$ of TNB with a short axis polarization.

Another result of this study is that the EDA complex crystal presents the molecular spectroscopist with a useful method for the investigation of *molecular* electronic structure. The advantages of crystal spectra are the directness of the measurements and the low ambiguity in assignments. At best, other methods for such large molecules can only produce relative assignments with nonnegligible uncertainties.

But crystal spectra can have severe drawbacks. The extremely complex spectra that arise from crystal interactions and perturbations often vitiate the certainty and precision of the assignments for complex molecules. To escape these, molecular spectroscopists have used mixed crystals where the host crystal is doped with the molecule to be studied. This requires an assumption regarding the guest's orientation in the host lattice. Further, the guest distribution is assumed to be homogeneous and guest concentrations must be known. The host and guest must be compatible and not completely overlap in their absorptions.

The A-TNB crystal indicates that these problems may be avoided. The crystal structure of the complex will leave no uncertainty regarding molecular orientation. Crystals may be grown and recrystallized without fear of widely varying their properties. Further, several complexes of a given molecule can be made to produce environmental perturbations or to determine a needed region of the spectrum should some part of it be dominated by the component not being studied.

While the overlap of bands can also be a great problem, the EDA complex can be employed effectively by selecting an acceptor, say, with symmetry-determined polarizations. Because these are known along with the molecule's orientation, the acceptor spectrum can be subtracted out, leaving the spectrum of the donor. Thus, aside from their intrinsic interest as an important class of compounds, EDA complex crystals are attractive for use as spectroscopic matrices.

Acknowledgment. This work was supported in part by NSF Grant DMR-76-11634.

References and Notes

- (1) C. J. Eckhardt and R. R. Pennelly, *J. Am. Chem. Soc.*, **98**, 2034 (1976).
- (2) C. J. Eckhardt and J. Merski, *Surf. Sci.*, **37**, 937 (1973).

- (3) C. J. Eckhardt and R. J. Hood, *J. Am. Chem. Soc.*, **101**, 6170 (1979).
 (4) J. Merski and C. J. Eckhardt, *J. Chem. Phys.*, to be submitted.
 (5) D. Haarer, *Chem. Phys. Lett.*, **27**, 21 (1974); **31**, 192 (1975).
 (6) D. Haarer, M. R. Philpott, and H. Morawitz, *J. Chem. Phys.*, **63**, 5238 (1975).
 (7) S. P. McGlynn and J. D. Boggus, *J. Am. Chem. Soc.*, **80**, 5096 (1958).
 (8) S. P. McGlynn, J. D. Boggus, and E. Elder, *J. Chem. Phys.*, **32**, 357 (1960).
 (9) J. Czekalla, A. Schmillen, and K. J. Mager, *Z. Elektrochem.*, **61**, 1053 (1957); **63**, 623 (1959).
 (10) S. K. Lower, R. M. Hochstrasser, and C. Reid, *Mol. Phys.*, **4**, 161 (1961); J. Tanaka and K. Yoshihara, *Bull. Chem. Soc. Jpn.*, **38**, 739 (1965).
 (11) R. M. Hochstrasser, S. K. Lower, and C. Reid, *J. Mol. Spectrosc.*, **15**, 257 (1965); *J. Chem. Phys.*, **41**, 1073 (1964).
 (12) R. S. Mulliken and W. B. Person, "Molecular Complexes", Wiley-Interscience, New York, 1969, p 127.
 (13) B. G. Anex and L. J. Parkhurst, *J. Am. Chem. Soc.*, **85**, 3301 (1963).
 (14) B. Chakrabarti and S. Basu, *J. Chem. Phys.*, **63**, 1044 (1966); J. Yarwood, Ed., "Spectroscopy and Structure of Molecular Complexes", Plenum Press, New York, 1973.
 (15) B. G. Anex and A. V. Fratini, *J. Mol. Spectrosc.*, **14**, 1 (1964); B. G. Anex, *Mol. Cryst. Liq. Cryst.*, **1**, 1 (1966).
 (16) D. Brown, S. C. Wallwork, and A. Wilson, *Acta Crystallogr.*, **17**, 168 (1964).
 (17) Because the measured intensity is proportional to the square of the cosine at the angle that the transition moment makes to a given principal direction, a sign ambiguity obtains in the determination of that angle from measured intensities.
 (18) G. Briegleb, "Elektronen-Donator-Acceptor-Komplexe", Springer-Verlag, West Berlin, 1961.
 (19) M. Tamres, *J. Am. Chem. Soc.*, **65**, 654 (1961).
 (20) A. Bier, *Recl. Trav. Chim. Pays-Bas*, **75**, 866 (1956).
 (21) W. B. Person, *J. Am. Chem. Soc.*, **87**, 167 (1965).
 (22) H. W. Offen, *J. Chem. Phys.*, **42**, 430 (1965).
 (23) T. E. Peacock, "Electronic Properties of Aromatic and Heterocyclic Molecules", Academic Press, New York, 1965, Chapter 8.
 (24) F. H. Herbst, "Perspectives in Structural Chemistry", Vol. IV, J. D. Dunitz and J. A. Ibers, Eds., Wiley, New York, 1971.
 (25) J. R. Hoyland and L. Goodman, *J. Chem. Phys.*, **36**, 12 (1962).
 (26) P. A. Clark, F. Brogli, and E. Heilbronner, *Helv. Chim. Acta*, **55**, 1415 (1972).
 (27) E. P. Krainov, *Opt. Spectrosc. (USSR)*, **16**, 532 (1964).
 (28) J. N. Murrell, "The Theory of Electronic Spectra of Organic Molecules", Wiley, New York, 1963, Chapter 6.
 (29) L. E. Lyons and L. J. Warren, *Aust. J. Chem.*, **25**, 1411, 1427 (1972).
 (30) T. E. Peacock and P. T. Wilkinson, *Proc. Phys. Soc., London*, **83**, 355 (1964).
 (31) P. H. H. Fischer and C. A. McDowell, *Mol. Phys.*, **8**, 357 (1964).

Infrared Spectra of Hydrogen-Bonded π Complexes between Hydrogen Halides and Acetylene

Stephen A. McDonald, Gary L. Johnson, Brian W. Keelan, and Lester Andrews*

Contribution from the Chemistry Department, University of Virginia, Charlottesville, Virginia 22901. Received October 9, 1979

Abstract: Hydrogen-bonded π complexes $C_2H_2 \cdots H-X$ have been formed by codeposition of C_2H_2 and HX in excess argon at 15 K and by vacuum-UV photolysis of vinyl halides. The strength of the hydrogen bond, as measured by the displacement of the $H-X$ vibrational fundamental below the isolated HX value, decreases in the series HF , HCl , and HBr as expected. Similar complexes made from di- and trichloroethylenes give slightly higher $H-Cl$ vibrations which show minimal interaction between the halide and the acetylene substituent. The $H-F$ fundamentals for C_2H_4 and C_2H_2 complexes at 3732 and 3747 cm^{-1} , respectively, show that the π electrons in double and triple bonds are comparable hydrogen-bond acceptors.

Introduction

Hydrogen bonding is of significant interest owing to its physical and biological importance. The traditional view of the hydrogen-bonding interaction has been expanded to include many electron-rich systems as the donor species, and in the past decade some experimental and theoretical work has been done on hydrogen-bonding π -electron complexes.¹⁻³ The present study focuses on the H bond formed between acetylene and hydrogen halide molecules HX ($X = F, Cl, Br$) through its effect on the $H-X$ stretching vibration.

Recent matrix isolation work has characterized the neutral hydrogen-bonding complexes $CH_3 \cdots H-F$ and $CH_3F \cdots H-F$ by $H-F$ stretching modes at 3764 and 3774 cm^{-1} , respectively,^{4,5} and the charged complexes $(F-H \cdots CF_2)^-$ and $(F-H \cdots CHF)^-$ by $H-F$ fundamentals at 3562 and 3124 cm^{-1} , respectively.^{6,7} In contrast, the HF diatomic fundamental is at 3962 cm^{-1} in solid argon.⁸ The displacement of the $H-F$ stretching mode to lower frequency is a measure of the strength of the H bond in the complex,⁹ and the large shifts observed for the charged complexes may help determine the electron distribution in these anions.

Hydrogen halide-acetylene or olefin complexes of the type studied here are possible intermediates in addition reactions of these materials. Hydrogen chloride infrared laser emission has been observed following vacuum-UV photolysis of dichloroethylenes in the gas phase, and the isomeric form of the precursor was found to influence the population of HCl vibrational levels.¹⁰ Parallel studies of the vacuum-UV photolysis

of dihaloethylenes during condensation in solid argon trapped a complex of HX and $HC \equiv CX$, which is probably a primary photolysis product. Here follows an experimental study of the synthesis and spectroscopy of π complexes between acetylene and hydrogen halides.

Experimental Section

Acetylene-hydrogen halide complexes were formed by vacuum ultraviolet photolysis of haloethylenes and by codepositing hydrogen halides and acetylene with excess argon at 15 K. The cryogenic apparatus and the vacuum-UV photolysis technique have been described previously.^{11,12} The various substituted ethylenes, 1,1-dichloro-, *trans*-dichloro-, trichloro-, tetrachloro-, 1,2-dibromo-, vinyl bromide (Aldrich Chemical Co.), vinyl fluoride, *cis*-difluoro- (Peninsular Chemresearch), and vinyl chloride (Matheson) were purified through fractional distillation on a vacuum line. HF and DF were produced by the reaction of F_2 (Matheson) with H_2 (Air Products) or D_2 (Airco) at very low pressures in a stainless steel vacuum system. Hydrogen bromide, hydrogen chloride, and chlorine (Matheson) and deuterium chloride (Merck Sharpe and Dohme) were used as received. Acetylene (Matheson) and C_2D_2 (Merck Sharpe and Dohme) were frozen and evacuated to remove volatile impurities. *cis*-1,2-Dichloroethylene (Aldrich, 65%) was purified on a preparative gas chromatograph. *cis*- and *trans*-dichlorodideuterioethylene were prepared by reacting C_2D_2 with Cl_2 and separating the isomers on a gas chromatograph. *cis*- $C_2D_2F_2$ was formed by exchange with the hydrogen compound in $NaOD/D_2O$ at 90 °C for 2 days.¹³ Argon matrix gas (Air Products) was used without further purification.

Samples were diluted with argon ($Ar/sample = 400/1$) and deposited at 2-3 mM/h for about 12-18 h with 1048-1067-Å photolysis